JACC Vol. 19, No. 7
June 1992:1610–8

Origin of Arterial Wall Dissections Induced by Pulsed Excimer and Mid-Infrared Laser Ablation in the Pig

TON G. VAN LEEUWEN, MSc, LIESELOTTE VAN ERVEN, MD, JOHN H. MEERTENS, MASSOUD MOTAMEDI, PhD,* MARK J. POST, MD, PhD,† CORNELIUS BORST, MD, PhD, FACC

Utrecht, The Netherlands and Galveston, Texas

To study adjacent tissue damage after delivery of holmium, thulium and excimer laser pulses, porcine thoracic aortas were irradiated in vivo. After 3 days, microscopic analysis of 67 craters produced by all three lasers demonstrated large dissections extending from the craters. The mean diameter of the dissections was smaller for excimer-induced craters (1.38 ± 0.42 mm; n = 22) than for holmium-induced (2.7 ± 0.87 mm; n = 22) and thulium-induced (2.37 ± 0.42 mm; n = 14) craters ($p < 0.01$ vs. mid-infrared dissections). In addition, microscopic analysis demonstrated necrosis adjacent to the crater. The lateral necrotic zones of the thulium-induced craters were smaller than the holmium- and excimer-induced necrotic zones ($p < 0.01$).

To identify the origin of the excessive tissue tearing, laser-saline and laser-tissue interaction were compared in vitro by time-resolved flash photography. In saline solution, the mid-infrared lasers showed bubble formation on a microsecond time scale. The excimer laser produced similar bubbles in the vicinity of tissue. For all three lasers, elevation of the tissue surface was shown during in vitro ablation. Dimension (diameter up to 4 mm) and time course (rise time of 100 to 300 μs) of bubble formation and tissue elevation were strikingly similar.

Thus, tissue dissections are caused by the expansion of a vapor bubble within the target tissue. Coronary dissections after excimer and mid-infrared laser angioplasty might be related to the forceful bubble expansion.

(J Am Coll Cardiol 1992;19:1610–8)

The ability to deliver laser light through flexible fibers has led to the intravascular use of laser energy. Laser angioplasty has the potential to support or substitute for balloon angioplasty. The development of coronary laser angioplasty has focused on the use of the xenon chloride (XeCl) excimer laser (λ = 308 nm) (1–3) because this pulsed laser was reported (4) to be capable of precise tissue ablation with minimal adjacent tissue injury. Recent in vitro studies (5,6), however, demonstrated that the ablation process with excimer lasers is quite violent, which might explain the high incidence of dissections (although not flow limiting) after coronary laser angioplasty (7). In view of these findings, Neu et al. (8) made the important observation that during noncontact excimer ablation of aorta submerged in saline solution, a bubble formed on top of the tissue and expanded and collapsed within 200 μs. We reported (9,10) a similar phenomenon for the pulsed holmium laser interaction with saline solution and suggested that the rapid expansion of a water vapor bubble within the tissue might induce arterial wall dissections.

The ultraviolet light emitted by the excimer laser is strongly absorbed by protein molecules and nucleic acids (attenuation coefficient >10 mm^{-1}) (11). In contrast, mid-infrared laser light (λ = 1.9 to 2.1 μm) is strongly absorbed by water molecules. Thus, effective tissue ablation by pulsed mid-infrared lasers is achieved with little thermal damage to adjacent tissue (12–15). Mid-infrared lasers are solid state lasers that are inexpensive, reliable and easy to operate. For these reasons, they may offer an alternative to the excimer laser for coronary laser angioplasty (16). An advantage of the holmium:yttrium-aluminum-garnet (YAG) laser over the holmium:yttrium-laser may be the larger absorption coefficient of laser energy in water (6 vs. 3 mm^{-1}, respectively) (10). Different tissue absorption coefficients for the excimer and mid-infrared laser light are expressed in the clinically used laser variables (2,16) (for example, repetition rate and fluence). The extent of the adjacent tissue damage will also depend on the variables used.

The aim of this study was to compare the extent of adjacent mechanical and thermal tissue damage in the form of dissections and necrosis caused by mid-infrared (holmium:yttrium-scandium-gallium-garnet (YSGG) [λ = 2.09 μm] and thulium:YAG [λ = 2.01 μm]) laser and

From the Department of Cardiology, Heart Lung Institute, University Hospital Utrecht, Utrecht, The Netherlands; the *University of Texas, Galveston, Texas; and †Interuniversity Cardiology Institute of the Netherlands, Utrecht. Mr. van Leeuwen was supported by Grant 37.007 from the Netherlands Heart Foundation, The Hague, The Netherlands.

Manuscript received July 30, 1991; revised manuscript received November 13, 1991, accepted November 26, 1991.

Address for reprints: Ton G. van Leeuwen, Experimental Cardiology Laboratory, Room E02.562, University Hospital Utrecht, P.O. Box 85500, 3508 GA Utrecht, The Netherlands.

©1992 by the American College of Cardiology

0735-1097/92/$5.00

ultraviolet (XeCl excimer) laser ablation in vivo. In addition, we attempted to determine the mechanism responsible for the tissue ruptures reported (9,15,14,17) after mid-infrared laser ablation of aortic tissue in vitro.

Methods

Laser sources and delivery fibers. The experiments were performed with a mid-infrared laser (SchwartzElectroOptics) supplied with a holmium:YSGG (λ = 2.09 μm) or thulium: YAG (λ = 2.01 μm) laser rod and a XeCl excimer (λ = 308 nm) laser (Technolas MAX-10). The mid-infrared and ultraviolet laser pulses were detected with a fast pyroelectric element (Molectron Detector, P5-01) incorporated in a circuit with a rise time of 10 ns. The holmium laser pulse consisted of a 500-μs long series of μs spikes. The thulium laser pulse consisted of a 300-μs long series of about 25 laser spikes of 10 to 25 μs each. The full width at half maximum for both mid-infrared laser pulses was 200 μs. The length of the excimer laser pulse was 115 ns.

During in vivo experiments, the mid-infrared laser pulses were coupled into a low hydroxyl (OH) silica fiber (320-μm core diameter) with a 1-mm large aperture tip (Advanced Cardiovascular Systems). This lensed fiber tip expanded the laser beam over the entire front surface of the tip (18). During in vitro experiments, the pulse energy at the bare fiber tip (320-μm diameter) was varied from 100 to 700 mJ, resulting in fluences (energy per unit of area) at the fiber tip of 1.2 to 8.7 J/mm^2. To determine the effect of fluence, experiments were performed with a 600-μm diameter bare fiber tip. The energy was varied from 200 to 500 mJ/pulse (fluences 0.7 to 1.8 J/mm^2).

The low OH silica fibers used for optimal transmission of mid-infrared laser light were not appropriate for the excimer laser studies. To obtain in vivo results comparable with those of the 1-mm large aperture tip, the excimer laser pulses were coupled into a 900-μm diameter fiber with a 1.25-mm diameter ball tip, as described previously (19). In vitro experiments were performed with a 900-μm diameter bare fiber. The energy was varied from 13 to 40 mJ/pulse (fluences 20 to 63 mJ/mm^2).

In Vivo Experiments

Throughout the course of the experiment, animal care conformed to the "Position of the American Heart Association on Research Animal Use" adopted November 11, 1984.

Surgical procedure. Thirteen normal female Yorkshire-land race pigs weighing 28 to 40 kg were used in this study. After induction of anesthesia with Stresnil (azaperone, 3 mg/kg body weight) and Hypnodil (metomidate, 4 mg/kg), pigs were ventilated by means of a servo respirator with a mixture of oxygen and nitrous oxide with halothane (1% to 2%) added. The pigs received 100 IU/kg of heparin. Arterial blood pressure, heart rate and an electrocardiogram were continuously recorded during the operation and arterial blood gases were measured regularly. After a left thoracotomy in the fourth intercostal space, the superior lobe of the left lung was collapsed and the upper portion of the descending aorta was dissected over 6 to 7 cm. The aorta was cross-clamped and incised longitudinally over 4 cm to expose the intimal surface. After laser irradiation, the incision was closed with a continuous suture of 5-0 prolene and the clamp was gradually removed from the aorta to restore the body circulation without a severe decrease in blood pressure. During clamping, nitroprusside was infused at 0.3 mg/min. Just before unclamping, nitroprusside was replaced by a dobutamine infusion (0.1 to 0.02 mg/min). The thorax was closed and the lung was expanded.

Laser irradiation. The laser variables needed to create lesions with a depth of 0.7 to 1 mm were chosen in accordance with prior in vitro dosimetry studies. Mid-infrared laser-induced craters were produced by either two consecutive holmium laser pulses of 500 mJ (peak fluence 1.8 J/mm^2 per pulse, calculated by ray-tracing [19]) or two thulium laser pulses of 250 mJ (0.9 J/mm^2 per pulse) (19) through the 1-mm aperture tip. The repetition frequency was 1 Hz. Ultraviolet laser-induced craters were produced by 10 to 15 excimer laser pulses of 25 mJ (39 mJ/mm^2) delivered through the 1.25-mm ball tip at 10 Hz. During the in vivo experiments, the fiber tip was clamped in a steelyard to deliver and record a force of 0.5 N (50 g) perpendicular to the lumen side of the aorta. The fiber tip was in contact with the target tissue, which was submerged in a layer of saline solution. The energy at the fiber tips was measured by an external power meter before and after the surgical procedure.

Sacrifice and microscopic evaluation. Animals were killed 3 days after the operation after use of the same surgical approach just described. The aorta was punctured and clamped just proximal and distal to the segment containing the lesions. The segment containing the lesions was isolated and rinsed with a saline infusion, followed by perfusion-fixation for 2 h with 4% formalin, both at physiologic pressure. After the aorta was clamped, the animals were killed with intracardiac potassium chloride (20 mmol).

After excision and postfixation for ≥24 h, the lesions were processed for light microscopy. Transverse sections of the lesions were cut serially at intervals of 80 μm and stained with hematoxylin-eosin. Selected sections were also stained with elastin van Gieson. In the section containing the maximal lesion, the extent of the induced damage and necrosis was measured microscopically with a calibrated eyepiece. Wall necrosis was identified by the absence of cell nucleus staining in the hematoxylin-eosin section.

In Vitro Experiments

The interaction of the laser pulses with saline solution or tissue was investigated with time-resolved flash photography, as described previously (9). At an adjustable period of

JACC Vol. 19, No. 7
June 1992:1610–8

time after the start of the laser pulse, a flash lamp was triggered. During the light flash (25 μs), the charged control device chip of the video camera was exposed, freezing fast ablation and evaporation processes at appropriate moments.

Laser-saline solution interaction. A previous study (10) demonstrated that a water vapor bubble formed during holmium and thulium laser interaction with fluid. With the 320-μm diameter bare fiber tip submerged in saline solution, the diameter of the bubble was measured as a function of the delivered energy (100 to 700 mJ/pulse). Because of the low absorption of excimer laser light by water, no vapor bubble forms. However, if an absorber for the excimer laser light is present (for example, hemoglobin or tissue), bubble formation is possible, as described by Isner et al. (20) and van Leeuwen et al. (9).

Laser-tissue interaction: mid-infrared laser. We anticipated that vapor bubbles would form within tissue and could be observed as a tissue surface elevation during irradiation. To visualize the postulated rise of the intimal surface of porcine aorta, the surface was photographed at a 10° grazing angle. The bare fiber tip was positioned perpendicular to and in light contact with the target tissue, which was submerged in saline solution. The maximal diameter and height of the elevated tissue zone during the first, second and third laser pulses were measured as a function of the delivered energy of the holmium laser pulse (100 to 700 mJ/pulse, 1.2 to 8.7 J/mm^2).

To extrapolate the energies delivered by the 320-μm diameter fiber to clinically used fluences, holmium laser experiments were performed at equal energy per pulse with fiber tips of different sizes. Tissue elevation was measured with a 600-μm diameter fiber tip (200 to 500 mJ/pulse, 0.7 to 1.8 J/mm^2) and with the 1-mm large aperture tip (500 mJ/pulse, peak fluence 1.8 J/mm^2). To determine whether tissue water or water from the saline environment was vaporized during the pulse, experiments were also performed in air.

Laser-tissue interaction: excimer laser. No vapor bubble was formed by interaction of the laser light and saline solution. Therefore, the effect of the excimer laser pulse on porcine aorta was compared in light contact (no force) and in force contact. In the latter, the bare fiber tip was positioned perpendicular to the tissue with a force of 0.1 *N* (10 g). The laser energy delivered through a 900-μm diameter fiber was varied from 13 to 40 mJ/pulse (20 to 63 mJ/mm^2).

Statistical analysis. Data are presented as mean values ± SD. Mean values were compared by using one-way analysis of variance. Pairs of groups that differed significantly were denoted by a Duncan procedure. Differences were considered significant at $p < 0.05$.

Results

In Vivo Experiments

Dissections and craters. Microscopic analysis of laser-induced craters showed dissections extending from the crater wall that ran parallel to the intimal surface (Fig. 1). All three lasers produced these dissections, which were clearly visible by the dark staining of blood filling the dissections. The diameter of the dissections, including the crater width, was larger for the mid-infrared laser than for the excimer laser ($p < 0.01$) (Table 1). There was no correlation between the depth of the crater and the diameter of the dissections. The craters were partly filled with thrombus, containing leukocytes and erythrocytes.

Necrotic zone. Adjacent to the crater, a zone of necrotic tissue was observed. The thickness of the necrotic zone depended on the laser used. The rank order for the thickness of the necrotic zone at the bottom of the crater was: excimer < thulium < holmium ($p < 0.01$). The thickness of the necrotic zone lateral to the crater was smaller for the thulium laser than for the holmium and the excimer laser ($p < 0.01$). For all lasers, little necrosis (<40 μm) was observed in the tissue bordering the dissections. The dimensions of the craters, the dissections and the necrotic zones are presented in Table 1.

In Vitro Experiments

Laser-saline solution interaction: mid-infrared laser. In saline solution during a holmium and thulium laser pulse, a water vapor bubble was formed around the fiber tip. The bubble reached its maximal volume at 200 to 300 μs after the start of the laser pulse. After collapse (at 300 to 500 μs), the bubble again expanded and finally collapsed at about 600 to 900 μs. The bubble was pear-shaped (Fig. 2, top). The maximal diameter of the holmium-induced bubble increased with increasing energy (Fig. 3). In saline solution, the diameter of the bubble created by a 500-mJ holmium and 250-mJ thulium laser pulse through the large aperture tip was 3 ± 0.1 (n = 3) and 3.5 ± 0.1 mm (n = 3), respectively.

Laser-tissue interaction: mid-infrared laser. With the 320-μm diameter bare fiber tip in contact with the intimal surface of porcine aorta, an increase in tissue height was observed during and after delivery of the holmium and the thulium laser pulse. Figure 2 illustrates the relation, in time and size, between tissue elevation and the expansion of the vapor bubble in saline solution for a holmium laser pulse. The maximal diameter and height of the tissue elevation were reached at approximately 300 to 400 μs. The collapse of the tissue at 2 to 3 ms, however, was slower and later than the collapse of the vapor bubble in saline solution. Because of sticking of the aortic tissue to the 320-μm diameter fiber, the tissue did not return to its original position (Fig. 2, bottom).

During one holmium laser pulse, both the maximal height and the diameter of the elevated surface increased with the delivered energy (Fig. 3). In addition, the diameter of the elevated zone increased during the second consecutive laser

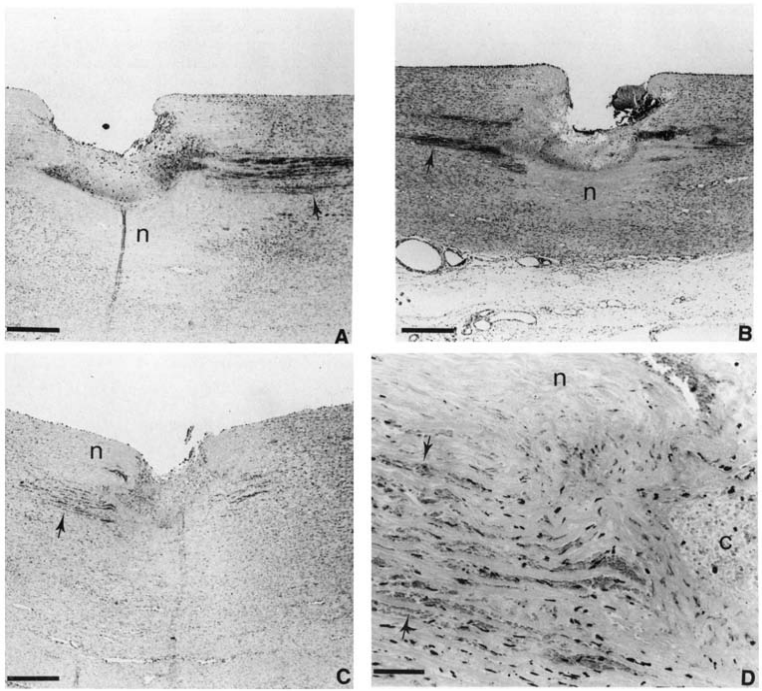

pulse. An apparent steady state was reached at the third pulse (Fig. 4).

Delivering a 200- to 500-mJ holmium laser pulse through a 600-μm instead of a 320-μm diameter fiber caused a fluence decrease by a factor of 3.5. However, the maximal diameter of the elevated tissue decreased by a factor of only 1.25 (Fig. 3). The maximal diameter of the elevated tissue due to the first and second 500-mJ holmium laser pulse delivered through the large aperture tip was 1.8 ± 0.3 (n = 10) and 2.4 ± 0.2 (n = 10) mm, respectively. Tissue elevation measurements were not repeated with the thulium laser pulses delivered through the 600-μm diameter fiber and large

Figure 1. Representative microscopic sections (hematoxylin-eosin stain) of craters and adjacent wall damage in porcine aorta after 3 days of survival (**A**, **B** and **C** ×50; **D** ×320, all reduced by 28%). The dissections parallel to the intimal surface (**arrows**) are identified by the dark staining of red blood cells. Note the necrotic zone (n) at the bottom of the crater in **A** and **B** and lateral to all craters. **A**, Crater after two consecutive holmium laser pulses (500 mJ/pulse, 1 Hz, 1-mm diameter large aperture fiber tip, **bar** = 300 μm). **B**, Crater after two consecutive thulium laser pulses (250 mJ/pulse, 1 Hz, 1-mm diameter large aperture fiber tip, **bar** = 300 μm). **C**, Crater after 15 excimer laser pulses (25 mJ/pulse, 10 Hz, 1.25-mm diameter ball tip on a 900-μm diameter fiber, **bar** = 300 μm). **D**, High power photomicrograph of the edge of the excimer-induced crater shown in C. Note the red blood cells in the dissections (**bar** = 50 μm).

Table 1. Quantitative Data for Craters After 3 Days of Survival

Laser Type	No.	Crater Size (mm)		Necrotic Zone (mm)		Diameter (mm) of the Dissections (no.)
		Depth	Width	Bottom (no.)	Lateral (no.)	
Holmium	29	0.96 ± 0.28	0.95 ± 0.36	0.43 ± 0.15 (20) *	0.36 ± 0.21 (24) *	2.70 ± 0.87 (22)
Thulium	14	0.67 ± 0.13	1.14 ± 0.29	0.31 ± 0.1 (14) *	0.17 ± 0.05 (14) *	2.37 ± 0.42 (14) *
Excimer	23	0.63 ± 0.23	0.69 ± 0.16	0.08 ± 0.05 (23) *	0.35 ± 0.09 (23) *	1.38 ± 0.41 (22) *

*Statistically significant difference ($p < 0.01$). All data are shown as mean value ± SD. Numbers in parentheses represent the number of measurements made.

aperture tip. For both lasers, intimal surface elevation was observed in air as well as in saline solution.

Laser-tissue interaction: excimer laser. The interaction between the excimer laser pulse and aorta in light contact mode showed a hemispheric vapor bubble on top of the tissue surface (Fig. 5, top). For a 34-mJ excimer laser pulse delivered through a 900-μm diameter bare fiber tip, the maximal diameter of this bubble was 2.5 ± 0.2 mm (n = 8). The maximal volume was reached at 100 μs. After collapse at 200 μs, the bubble expanded again and finally collapsed. Some small bubbles remained long after the pulse and rose to the surface of the saline solution.

With the fiber tip in contact with tissue with a force of 0.1 *N* (10 g), the hemispheric bubble was observed only during the 1st 5 to 10 laser pulses. As soon as the fiber tip had penetrated into the tissue, visible bubble formation was replaced by tissue elevation (Fig. 5, bottom). At approximately 100 μs, the maximal diameter of tissue elevation was reached. The tissue returned to its position at 400 to 500 μs. A vapor bubble that escaped through the interface of fiber and tissue at 100 μs did not dissolve.

The relation between the delivered energy per pulse through the 900-μm diameter fiber and the diameter of the hemispheric vapor bubbles and tissue elevations is presented in Figure 6. Both the vapor bubble and tissue elevation increased with increasing energy.

Discussion

The aim of this study was to compare the extent of adjacent tissue damage (mechanical and thermal) caused by mid-infrared and ultraviolet laser ablation in vivo and determine the mechanism responsible for the tissue ruptures reported after in vitro mid-infrared laser ablation of aortic tissue. Our principal findings were that both mid-infrared (holmium and thulium) and ultraviolet (XeCl excimer) laser ablation cause 1) adjacent tissue damage in the form of dissections extending over 1 mm from the crater wall and a lateral necrotic zone extending several hundred micrometers

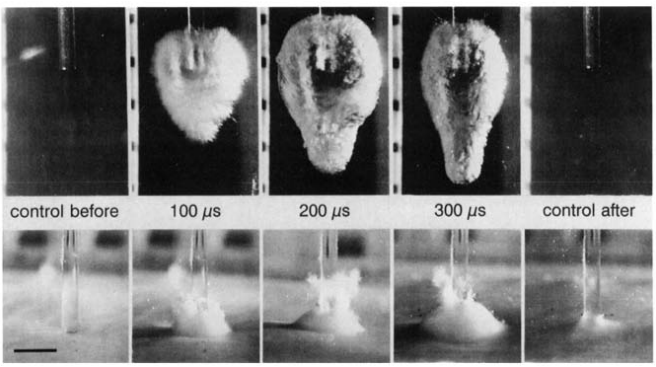

Figure 2. Photographs of the holmium laser-saline solution (**top**) and holmium laser-tissue (**bottom**) interaction before, during and after delivery of the 500-mJ holmium laser pulse. With the 320-μm diameter fiber tip submerged in saline solution (**top**), a pear-shaped water vapor bubble is formed. With the fiber tip in light contact with the porcine aorta submerged in saline solution (**bottom**), corresponding tissue elevation is observed (**bar** = 1 mm).

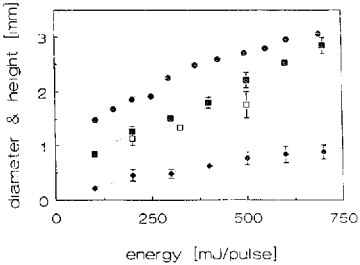

Figure 3. Maximal diameter of a vapor bubble induced in saline solution (●) by holmium laser pulses and maximal diameter (■) and height (◆) of the elevated intimal surface of porcine aorta at the first pulse as a function of the holmium energy delivered per pulse through a 320-μm bare fiber tip. Maximal diameters of the surface that was elevated by delivery of a 200- to 500-mJ holmium laser pulse through a 600-μm bare fiber tip are inserted (□). All data are shown as mean value ± SD (n = 8 per point).

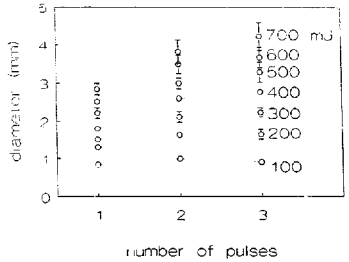

Figure 4. Maximal diameter of the elevated intimal surface of porcine aorta after delivery of one, two and three holmium laser pulses. Laser pulses were delivered in saline solution through a 320-μm diameter bare fiber tip.

in the surrounding tissue, and 2) large vapor bubbles. The expansion of a vapor bubble within tissue was deduced from tissue surface elevation.

Adjacent tissue damage: dissections. All three lasers produced considerable adjacent tissue damage, with minor differences among the lasers. The most striking phenomenon was the presence of dissections in the aortic wall. The size of these dissections may be exaggerated in this study because the craters were produced perpendicular to the intimal surface of the thoracic aorta and the dissections might be created more easily between its elastic lamellae than in muscular arteries. Preliminary findings suggest that the mechanical properties of the tissue may affect the extent but not the presence of the surface elevation and the tissue tearing. In this respect, it is interesting that dissections, although not flow limiting, are a relatively frequent complication of excimer and holmium laser angioplasty, with reported incidence rates of 12.1% and 28%, respectively (21,22).

We infer that the dissections are due to the forceful expansion of a vapor bubble within tissue when pulsed lasers are used. First, we observed tissue elevation during in vitro ablation of tissue as the missing link between the bubbles seen in saline solution and blood and the aortic wall dissections observed in vivo. The dimensions, their dependence on pulse energy and temporal course were strikingly similar for bubble formation and tissue elevation. Moreover, the diameters of the dissections, although subject to a large variation, were in accordance with the diameters of the bubbles and tissue elevation (Table 2). Second, although the mechanism of bubble formation is different for the infrared and ultraviolet lasers, the phenomena observed are similar. For the mid-infrared laser, tissue elevation was also observed in an air environment, indicating that it is tissue water rather than surrounding water that is evaporated. The chromophores for ultraviolet laser ablation are protein and nucleic acids, not water. We speculate that the origin of the excimer laser-induced bubble is twofold: 1) tissue pyrolysis produces volatile short chain hydrocarbons (for example, methane, acetylene and ethane) (23), and 2) the hot crater surface dissipates heat to neighboring water that evaporates (11).

Tissue dissections have been attributed to acoustic damage by shock waves (with velocities >1,500 m/s) caused by the absorption of high peak power laser pulses (17). From the temporal course of the tissue elevation, however, we estimate that the tissue elevation velocity was 10 to 30 m/s. As a result, tissue elevation cannot be due to a shock wave. In a previous study (9), we measured only small acoustic signals at the start of the holmium laser pulse. The most intense signals in saline solution were recorded at the time of collapse of the bubble. In the present study, the lifetime of the tissue elevation was increased compared with the lifetime of the vapor bubble, indicating that the bubble collapse was retarded by the surrounding tissue (24). These findings, the onset of tissue elevation just after the start of the laser pulse and the spatial and temporal correspondence of the tissue elevation with the bubble formation in saline solution led to the conclusion that vapor bubble expansion within the tissue causes tissue elevation and dissections. This view is in agreement with the recent observations of Chen and Israelachvili (25), who demonstrated that damage could also result during the formation of a bubble.

Vapor bubbles are likely to occur in the clinical situation because all three lasers produce these bubbles in blood. Moreover, Gijsbers et al. (6) reported that vapor bubble formation is not avoided with a long (220-ns) excimer laser pulse.

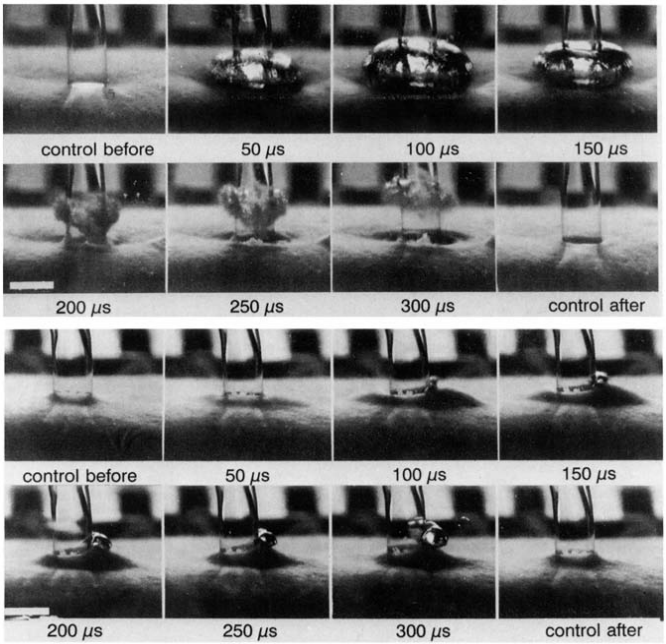

Figure 5. Time-resolved photographs of the interaction between a 34-mJ (53-mJ/mm²) excimer laser pulse in light contact mode (**top**) and with the 900-μm diameter fiber tip buried in the porcine aorta as a result of force contact (0.1 *N*) (**bottom**) (**bar** = 1 mm).

Apart from the expanding and imploding bubbles, we observed long-lived bubbles. We speculate that their contents are volatile short chain hydrocarbons, as described by Clarke et al. (23). The clinical effects of the long-lived vapor bubbles, which were only observed after excimer laser ablation, remain to be studied.

Adjacent tissue damage; necrosis. Although the craters produced in vivo in the thoracic aorta of the pig were intentionally similar for the three lasers, some differences were observed in the amount of necrosis surrounding the craters. The lateral necrotic zone was larger for the holmium than for the thulium laser (Table 1), an observation that corresponds to the smaller penetration depth in water of thulium laser light (0.16 mm) compared with that of holmium laser light (0.33 mm) (10). The smaller penetration depth resulted in a reduced zone of nonablative laser energy and may be advantageous for clinical application because the lateral zone is the remaining part of the tissue after laser angioplasty. The thickness of the necrotic zone at the bottom of the crater is in accordance with measurements for holmium- and thulium-induced craters reported by Nishioka and Domankevitz (12).

The necrotic zone at the bottom of the crater was minimal for the excimer laser compared with that of the mid-infrared laser. In contrast, the thickness of the necrotic zone at the lateral side of the crater was significantly larger ($p < 0.01$) than that for the thulium laser. This relatively large lateral necrotic zone after excimer ablation is probably due to heat accumulation by multiple laser pulses. In air, Gijsbers et al. (26) recorded an increase in tissue temperature up to 66 ± 7°C after excimer ablation of porcine aorta in vitro at 20 Hz.

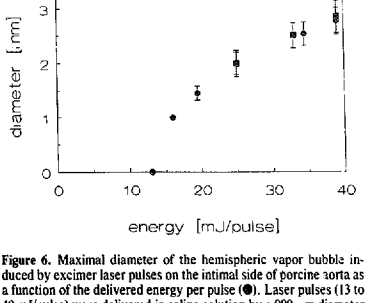

Figure 6. Maximal diameter of the hemispheric vapor bubble induced by excimer laser pulses on the intimal side of porcine aorta as a function of the delivered energy per pulse (●). Laser pulses (13 to 40 mJ/pulse) were delivered in saline solution by a 900-μm diameter fiber (20 to 63 mJ/mm²) in light contact with the tissue. Maximal diameter of tissue elevation as a function of the delivered energy at the fiber tip (■). Laser pulses were delivered through a 900-μm diameter fiber tip in force contact (0.1 *N*) with porcine aorta. All data are shown as mean value ± SD (n = 10).

These findings suggest that not only the difference in tissue absorption coefficients, but also the difference in the laser variables might have influenced the extent of adjacent tissue damage.

Relation between fluence and bubble formation. To minimize the influence of the fiber tip on the tissue elevation (for example, by friction), almost all mid-infrared experiments were performed with small diameter fiber tips in light contact with the tissue. Consequently, the fluence (1.2 to 8.7 J/mm² per pulse) was high compared with that used in clinical mid-infrared laser angioplasty (300 to 500 mJ/pulse, 0.5 to 0.8 J/mm²) (16). The experiments performed with a 600-μm diameter fiber demonstrated that changes in fluence had relatively little effect on bubble dimensions and the diameter of tissue elevation. Thus, these results suggest that for mid-infrared lasers, the diameter of the bubble and of tissue elevation was correlated with the energy per pulse.

Clinical implications. Among the various pulsed lasers, no essential difference in the impact on tissue was found. Both excimer and mid-infrared laser ablation was accompanied by vapor bubble expansion into the tissue, leading to substantial dissections. Although the size of the dissections with the excimer laser were smaller than with the infrared laser, they were prominent. Increasing the power, to ablate calcified plaque for instance, will also increase the dissection size. The creation of dissections and adjacent tissue necrosis during clinical application of these lasers in human atherosclerotic arteries remains to be demonstrated. It is likely that both the mid-infrared laser pulse (due to absorption by water) and the excimer laser pulse (due to absorption by hemoglobin and proteins) will induce bubble formation in blood and tissue. The expanding vapor bubble, however, will seek the path of least resistance and it is conceivable that this path is the cleavage plane between the plaque and the media. The relatively high incidence of dissections may reflect in vivo bubble expansion (7).

Table 2. Comparison Between In Vivo and In Vitro Diameters

Laser Type	Bubbles (mm)	Tissue Elevation (mm)	Dissections (mm)
Holmium*	3.0 ± 0.1 (3)	2.4 ± 0.2 (10)	2.7 ± 0.9 (22)
Thulium*	3.5 ± 0.1 (3)	Not measured	2.4 ± 0.4 (14)
Excimer†	2.0 ± 0.2 (10)	2.0 ± 0.2 (10)	1.4 ± 0.4 (22)

*Two laser pulses delivered through the 1-mm large aperture tip. †Ten to 15 laser pulses of 25-mJ each (∼ mJ/mm²) delivered through a 900-μm diameter fiber. Diameters are represented as mean ± SD. Numbers in parentheses represent the number of measurements made.

Conclusions. During tissue ablation, mid-infrared (holmium and thulium) lasers as well as ultraviolet (excimer) lasers create a vapor bubble that may expand into adjacent tissue. The forceful expansion of this bubble induces mechanical damage in adjacent tissue in the form of dissections. Whether these bubbles are related to the relatively high incidence of coronary dissections after excimer and mid-infrared laser angioplasty and whether these dissections affect the acute results and subsequent wall healing (restenosis rate) remain to be studied.

We thank Rudolf Verdaasdonk and Geert Gijsbers for fruitful discussion and Evelyn Velema for histologic and biotechnical assistance.

References

1. Sanborn TA, Torre SR, Sharma SK, et al. Percutaneous coronary excimer laser-assisted balloon angioplasty: initial clinical and quantitative angiographic results in 50 patients. J Am Coll Cardiol 1991;17:94–9.
2. Litvack F, Eigler NL, Margolis JR, et al. Percutaneous excimer laser coronary angioplasty. Am J Cardiol 1990;66:1027–32.
3. Karsch KR, Haase KK, Voelker W, Baumbach A, Mauser M, Seipel L. Percutaneous coronary excimer laser angioplasty in patients with stable and unstable angina pectoris: acute results and incidence of restenosis during 6-month follow-up. Circulation 1990;81:1849–59.
4. Gruentzig AR, Litvack F, Forrester JS, et al. Laser ablation of human atherosclerotic plaque without adjacent tissue injury. J Am Coll Cardiol 1985;5:929–33.
5. Srinivasan R, Casey KG, Haller JD. Subnanosecond probing of the ablation of soft plaque from arterial wall by 308 nm laser pulses delivered through a fiber. IEEE J Q E 1990;26:2279–83.
6. Gijsbers GHM, van den Broecke DG, van Wieringen N, Sprangers RLH, van Gemert MJC. 308 nm excimer laser ablation with a contact beam delivery system: effects of applied force and gaseous debris (abstr). Lasers Surg Med 1991;(suppl 3):15.
7. Isner JM. Laser angioplasty: state of the art (abstr). Lasers Surg Med 1991;(suppl 3):63.
8. Neu W, Nyga R, Tischler C, Haase KK, Karsch KR. Ultrafast imaging of vascular tissue ablation by a XeCl excimer laser. In: Abela GS, Katzir A, eds. Diagnostic and Therapeutic Cardiovascular Interventions. Bellingham WA: SPIE, 1991;1425:37–44.
9. van Leeuwen TG, van der Veen MJ, Verdaasdonk RM, Borst C. Non-contact tissue ablation by holmium:YSGG laser pulses in blood. Lasers Surg Med 1991;11:26–34.
10. van Leeuwen TG, Motamedi M, Verdaasdonk RM, Borst C. Interaction

of pulsed IR laser radiation with fluid: implication for tissue ablation (abstr). Lasers Surg Med 1991(suppl 3):16.
11. Ornevsky AA, Jacques SL, Saidi IS, et al. Optical properties and energy pathways during XeCl excimer laser irradiation of atherosclerotic aorta (abstr). Lasers Surg Med 1991(suppl 3):5
12. Nishioka NS, Domankevitz Y. Comparison of tissue ablation with pulsed holmium and thulium lasers. IEEE J Q E 1990;26:2271–5.
13. Trauner K, Nishioka N, Patel D. Pulsed holmium:yttrium-aluminum-garnet (Ho:YAG) laser ablation of fibrocartilage and articular cartilage. Am J Sports Med 1990;18:316–20.
14. Lilge L, Radtke W, Nishioka NS. Pulsed holmium laser ablation of cardiac valves. Lasers Surg Med 1989;9:458–64.
15. Schomacker KT, Domankevitz Y, Flotte TJ, Deutsch TF. Co:MgF2 laser ablation of tissue: effect of wavelength on ablation threshold and thermal damage. Lasers Surg Med 1991;11:141–51.
16. Geschwind HJ, Dubois Rande JL, Murphy Chutorian D, Tomaru T, Zelinsky R, Loisance D. Percutaneous coronary angioplasty with mid-infrared laser and a new multifibre catheter (letter). Lancet 1990;336: 245–6.
17. Bonner RF, Smith PD, Prevosti LG, Bartorelli A, Almagor Y, Leon MB. Laser sources for angioplasty. In: Abela GS, ed. Lasers in Cardiovascular Medicine and Surgery: Fundamentals and Techniques. Boston, Dordrecht, London: Kluwer Academic, 1990:31–44.
18. White CJ, Ramee SR, Collins TJ, Mesa JE, Paulsen DB, Murgo JP. Recanalization of arterial occlusions with a tapered fiber and a holmium: YAG laser. Lasers Surg Med 1991;11:250–6.
19. Verdaasdonk RM, Borst C. Ray tracing of optically modified fiber tips. I. Spherical probes. Applied Optics 1991;30:2159–71.
20. Isner JM, DeJesus SR, Clarke RH, Gal D, Rongione AJ, Donaldson RF. Mechanism of laser ablation in an absorbing fluid field. Lasers Surg Med 1988;8:543–54.
21. Litvack F. Excimer laser coronary angioplasty (abstr). Lasers Surg Med 1991(suppl 3):87.
22. Geschwind HJ, Kvasnicka J, Nakamura F, Zelinsky R, Dubois-Rande JL. Infrared laser coronary angioplasty: initial results (abstr). Med Tech 1991(suppl 2):9.
23. Clarke RH, Isner JM, Donaldson RF, Jones GL. Gas chromatographic-light microscopic correlative analysis of excimer laser photoablation of cardiovascular tissues: evidence for a thermal mechanism. Circ Res 1987;60:429–37.
24. Vogel A, Schweiger P, Frieser A, Asiyo MN, Birngruber R. Intraocular Nd:YAG laser surgery: light tissue interaction, damage range, and reduction of collateral effects. IEEE J Q E 1990 26:2240–60.
25. Chen YL, Israelachvili J. New mechanism of cavitation damage. Science 1991;252:1157–60.
26. Gijsbers GHM, Sprangers RLH, Keijzer M, et al. Some laser-tissue interactions in 308 nm excimer laser coronary angioplasty. J Intervent Cardiol 1990;3:231–41.